

# T2 phase site occupancies in the Cr–Si–B system: a combined synchrotron-XRD/first-principles study

Thiago T. Dorini<sup>a</sup>, Bruno X. de Freitas<sup>b</sup>, Pedro P. Ferreira<sup>b</sup>, Nabil Chaia<sup>b</sup>, Paulo A. Suzuki<sup>b</sup>, Jean-Marc Joubert<sup>c</sup>, Carlos A. Nunes<sup>b</sup>, Gilberto C. Coelho<sup>b</sup>, Luiz T. F. Eleno<sup>b,\*</sup>

<sup>a</sup>Université de Lorraine, CNRS, IJL, Nancy, France

<sup>b</sup>Computational Materials Science Group (ComputEEL/MatSci), Escola de Engenharia de Lorena da Universidade de São Paulo (EEL-USP), Materials Engineering Department (Demar), Lorena-SP, Brazil

<sup>c</sup>Univ. Paris Est Creteil, CNRS, ICMPE, UMR 7182, 2 rue Henri Dunant, 94320 Thiais, France

---

## Abstract

Boron and Silicon site occupancies of the T2 phase in the Cr–Si–B system were investigated experimentally and by first-principles electronic-structure calculations. A sample with nominal composition  $\text{Cr}_{0.625}\text{B}_{0.175}\text{Si}_{0.2}$  was arc-melted under argon, encapsulated in a quartz-tube and heat-treated at 1400°C for 96 hours. It was then analyzed using Scanning Electron Microscopy (SEM) and X-Ray Diffractometry (XRD) with synchrotron radiation. An excellent agreement was obtained between experiments and theoretical calculations, revealing that Si occupies preferably the  $4a$  sublattice of the structure, as boron atoms in  $8h$  nearest-neighbors form very stable *dumbbell* bonds. Site preferences are thus a key factor for the stabilization of the structure. The results of this work provide important information to support a better description of this phase in alloys with Si and B, since T2 phases are known to occur in many important Transition Metal–Si–B ternary systems, such as Nb/Mo/W/Ta/V–Si–B.

**Keywords:** X-ray diffraction (XRD), Density Functional Theory (DFT), Refractory metals, Cr-Si-B, Intermetallics

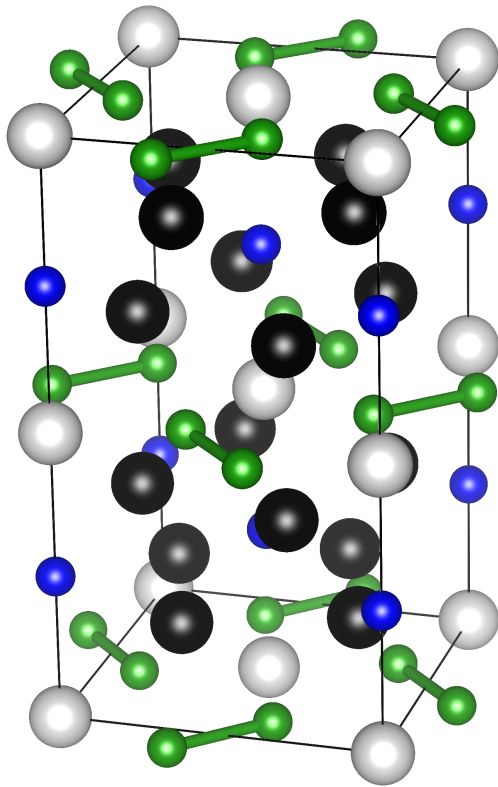
---

Recent demands for energy generation and consumption require the search for new materials and processing routes capable of stabilizing mechanical and thermal properties during long times under extreme conditions. For example, among the key materials for high temperature applications are multicomponent systems containing refractory metals (RM) such as Nb and Mo, often modified with Si and B [1–7], originating the so-called RM-silicides. However, these alloys are known to exhibit low to moderate resistance to oxidation/corrosion at elevated temperatures. If the modification of the alloy composition is not effective in enhancing the oxidation behavior at high temperatures, the deposition of protective coatings is required to ensure the integrity of parts during service [8–10]. Coatings developed in the past for this class of materials are based on silicide compounds that are able to form a silica protective layer during exposure [8, 11]. Additions of boron to silicides is of particular interest, leading to the modification of the silica layer by lowering its viscosity, which can help to heal fatigue cracks induced by thermal cycling. Therefore, knowledge of phase diagrams and the crystal structures associated with intermetallic phases present in RM–Si–B systems is very important to develop new compositions for alloys and coatings.

Among the key systems, Cr–Si–B is a promising candidate, especially alloys in the Cr-rich region [12–14]. Despite its potential in a wide range of applications, there is a lack of experimental and

---

\*Corresponding author: +55 12 3159 9810, website: <https://computeel.org>  
Email address: [luizeleleno@usp.br](mailto:luizeleleno@usp.br) (Luiz T. F. Eleno)



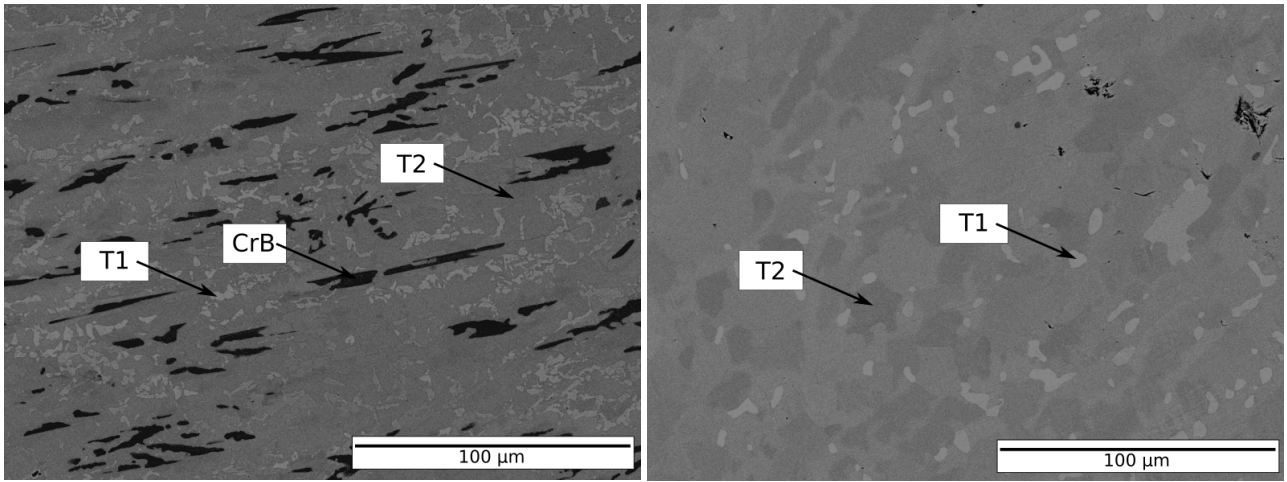
Prototype	Cr <sub>5</sub> B <sub>3</sub>	
Space group	<i>I4/mcm</i> (140)	
Pearson symbol	<i>tI32</i>	
Wyckoff positions:		
● Cr1	16 <i>l</i>	(.166, .666, .15)
○ Cr2	4 <i>c</i>	(0, 0, 0)
● B1	8 <i>h</i>	(.625, .125, 0)
● B2	4 <i>a</i>	(0, 0, <sup>1</sup> / <sub>4</sub> )

**Figure 1:** (a) Crystallographic information on the T2-Cr<sub>5</sub>B<sub>3</sub> compound [28, 29]. The only bonds shown are the *dumbbells* between two nearest-neighbor boron (8*h*) atoms.

theoretical data in the literature. In particular, the Cr-Si-B system contains a phase, usually denoted by T2 (which is a ternary extension of Cr<sub>5</sub>B<sub>3</sub> with silicon substitution for boron), with very scarce information regarding its site occupancies and enthalpy of formation.

Therefore, the aim of the present work is to determine the sublattice occupancies of the T2 compound using synchrotron X-ray diffraction measurements and Density Functional Theory (DFT) calculations in order to help to improve the reliability of Cr-Si-B thermodynamic descriptions. In the following discussion, we demonstrate that Si atoms, in fact, have a preference for one of the boron sublattices of the T2 phase, in contrast to what was proposed in the optimization performed by Villega [13]. That information calls for a new, appropriate thermodynamic reassessment of the Cr-Si-B system. In addition, besides providing invaluable information on the poorly-studied Cr-Si-B system, our work also sheds light on the need for better descriptions of related systems, as T2 phases are known to occur in many important ternaries, such as Nb/Mo/W/Ta/V-Si-B [15–27].

The tetragonal unit cell and crystallographic information on the T2-Cr<sub>5</sub>B<sub>3</sub> compound [28, 29] are presented in Fig. 1. Cr atoms occupy the 16*l* and 4*c* sites, while B occupies the 8*h* and 4*a* Wyckoff positions. From previous microanalysis experiments [13], Si dissolves in this boride by replacing B atoms, keeping the chromium content constant at a molar fraction of  $x_{\text{Cr}} = 0.625$ . A sample was then prepared with nominal composition Cr<sub>0.625</sub>B<sub>0.175</sub>Si<sub>0.2</sub>. It was obtained by arc melting of high-purity Cr (min. 99.9 wt%), Si (min. 99.99 wt%) and B (min 99.5 wt%) in a water-cooled copper crucible under analytical argon (min 99.995%) atmosphere. After the melting process, weight losses were lower than 1.3%. The sample was then encapsulated in a quartz tube under vacuum and heat-treated at 1400°C for 96h in a furnace with constant flow of analytical argon. The sample was characterized at room temperature through Scanning Electron Microscopy/Back-Scattered Electron Images (SEM/BSE) in the as-cast and heat-treated states, the latter being also submitted to XRD from synchrotron radia-



(a) As cast.

(b) Heat treated at 1400°C for 96h.

**Figure 2:** SEM images in BSE contrast of the  $\text{Cr}_{0.625}\text{B}_{0.175}\text{Si}_{0.2}$  sample, showing (a) the presence of CrB and T1- $\text{Cr}_5\text{Si}_3$  precipitates in a T2- $\text{Cr}_5(\text{Si},\text{B})_3$  matrix in the as-cast state, and (b) the microstructure after heat treatment at 1400°C for 96 h, with a two-phase microstructure constituted by T1 and T2.

tion. SEM/BSE micrographs were obtained from flat and polished specimens and XRD experiments were carried out in high resolution mode using a multiple axes Huber diffractometer located at the Brazilian Synchrotron Light Laboratory (LNLS) in Campinas (SP), Brazil. To improve randomness of orientation, the powder sample, sieved to below 53  $\mu\text{m}$ , was placed in a rotating 5 mm diameter-1 mm depth cylindrical support. The measurement was performed with a monochromatic X-ray beam ( $\lambda = 1.237 \text{ \AA}$ ). The combination of flat plate geometry and parallel beam gives results with a high peak/noise ratio, accurate enough to provide site occupancies with small standard deviations. Phase identification and refinement were performed using the Rietveld method [30, 31] with input crystallographic data from the literature [28, 32, 33].

Figs. 2a-b present a comparison of the as-cast and heat-treated  $\text{Cr}_{0.625}\text{B}_{0.175}\text{Si}_{0.2}$  sample. Clearly, during the heat treatment the CrB primary precipitates present in the as-cast sample are consumed, leading to larger amounts of the T1 ( $\text{Cr}_5\text{Si}_3$ ) and T2 ( $\text{Cr}_5(\text{Si},\text{B})_3$ ) phases in the heat-treated state, as predicted by Vilella [13]. Thus, the heat treatment at 1400°C for 96 h has led the system very close to thermodynamic equilibrium. Fig. 3 shows the XRD pattern of the heat-treated sample. All peaks were identified with the T1, T2 and a very small amount of remaining CrB phase not seen in the SEM image. Nowotny and Wittmann [12] proposed the existence of a  $\text{D}_{88}$  ternary phase at 1300°C, which was contested in the experimental investigations performed by Vilella [13] and Chad [14] at 1200°C, as the graphite crucible and low-purity boron (96.5 at%) used in Ref. [12] are suspected to stabilize the ternary phase. The present result establishes that the real equilibrium is the  $\text{Cr}_5\text{Si}_3$ - $\text{Cr}_5(\text{Si},\text{B})_3$ -CrB tie-triangle, showing, also at 1400°C, that the  $\text{D}_{88}$  phase is not stable in the Cr-Si-B system.

Site occupancies of Si and B were refined using the Rietveld method without any constraints on the composition. The only constraint was the full occupancy of the two sites ( $4a$  and  $8h$ ) possibly occupied by these two atoms. Therefore, besides the lattice constants, two parameters were refined, with  $\chi^2 = 3.9$  and  $R_B = 16.1\%$ . The Si occupancy on sites  $4a$  and  $8h$  is found to be 74(2) and 4(2)%, respectively, indicating a very strong preference of Si for site  $4a$ , with only a small fraction going to  $8h$ . These values correspond to 2.96 Si atoms in  $4a$  and 0.32 in  $8h$ , which are the values shown in Table 1. The refined composition was therefore  $x_{\text{Si}} = 0.102$ , in agreement with Vilella [13], who suggested a solubility of 9 at.% Si at 1400°C in the T2 phase. The Rietveld plot is shown in Fig. 3.

In order to support the experimental evidence, we performed *ab-initio* calculations considering

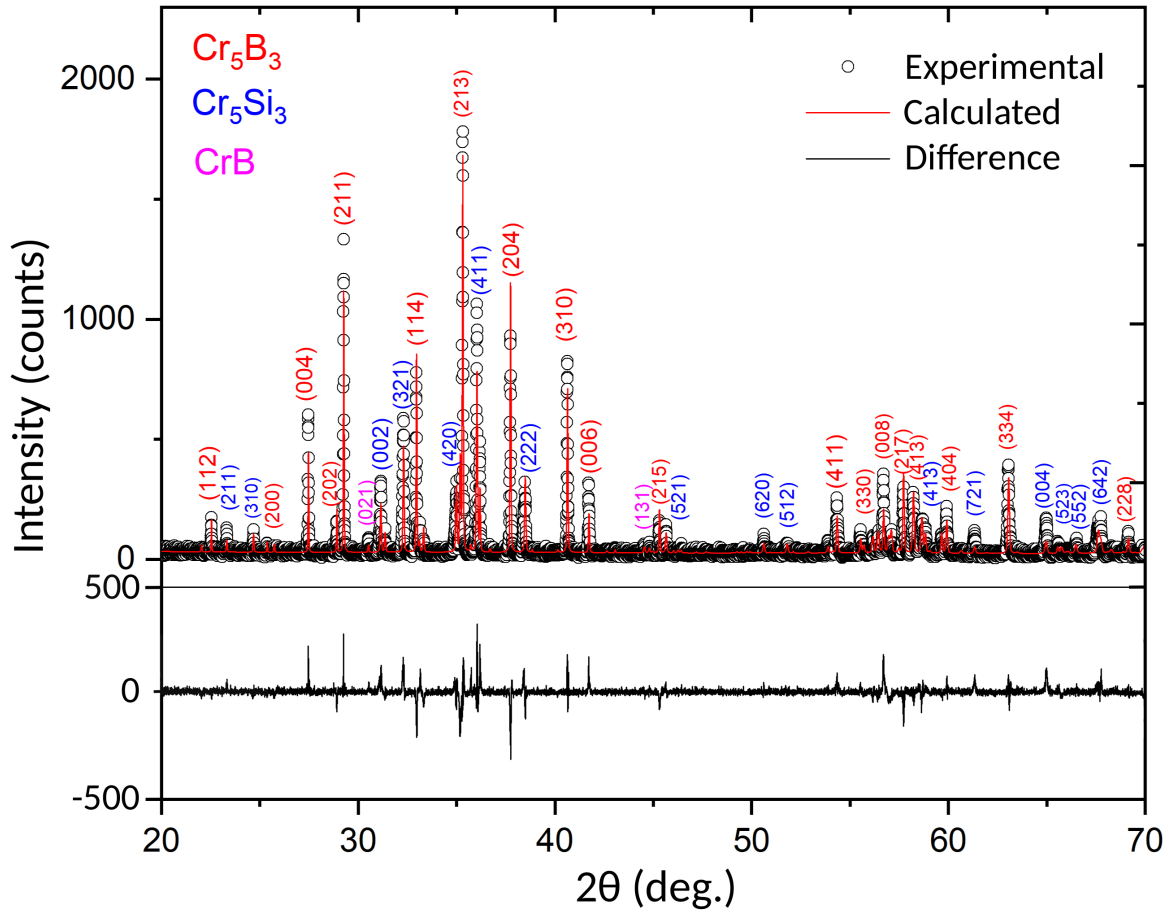


**Figure 3:** Synchrotron x-ray diffraction pattern of the  $\text{Cr}_{0.625}\text{B}_{0.175}\text{Si}_{0.2}$  sample heat-treated at  $1400^\circ\text{C}$  for 96 hours, showing the calculated intensities differences, using the Rietveld refinement, considering Si in both  $4a$  and  $8h$  sublattices.

the complete substitution of B by Si in the  $4a$  and  $8h$  sublattices, resulting in the ordered compounds and a few disordered compounds shown in Table 1, with mixing of Si and B in the same sublattice. The DFT [34, 35] calculations were then performed with the Quantum ESPRESSO code [36]. The Generalized Gradient Approximation (GGA) was used for the exchange and correlation (XC) functional with the Perdew-Burke-Ernzerhof (PBE) parametrization [37], considered appropriate for this class of materials [38–40]. A plane-wave cutoff energy of 190 Ry was used for all calculations, with a  $14 \times 14 \times 7$  Monkhorst–Pack grid [41]. All structures were fully relaxed with respect to lattice parameters and internal degrees of freedom, maintaining the space-group symmetry, by imposing a convergence limit of  $10^{-5}$  Ry in energy and  $10^{-3}$  Ry/au in interatomic forces for the ground-state.

Figures 4a-b present a comparison of experimental and calculated ground-state (0 K) lattice parameters ( $a$  and  $c$ ) obtained in the present work as a function of the Si molar fraction and B and Si site occupancies. The maximum difference between the results is approximately 2%, which may be attributed to the XC functional, since the GGA approximation tends to overestimate the forces between atoms, leading to smaller lattice parameters [42]. This difference can be duly noticed in Figs. 4a-b for both lattice parameters in the case of the Si-free compound (with only one exception for  $a$ ), when compared to the experimental data [43–45].

Fig. 4c shows the calculated formation enthalpies at 0 K for all compounds, obtained by the difference between the total energy of the structure and the total energies of the most stable phases of

**Table 1:** *Ab-initio* and experimental formation enthalpies and lattice parameters for compounds with different T2-structure occupations.

Compound	4a occ.	8h occ.	$x_{\text{Si}}$	$\Delta_f H$ (kJ/mol)	$a$ (nm)	$c$ (nm)
Cr <sub>5</sub> (B,Si) <sub>3</sub> (exp.)	1.04B/2.96Si	7.68B/0.32Si	0.102	—	0.56322(1)	1.04197(2)
Cr:(B) <sub>4a</sub> :(B) <sub>8h</sub>	4B	8B	0	−41.37	0.5414	1.0023
Cr:(B <sub>2</sub> Si <sub>2</sub> ) <sub>4a</sub> :(B) <sub>8h</sub>	2B/2Si	4B	0.0625	−39.13	0.5524	1.0124
Cr:(B) <sub>4a</sub> :(B <sub>6</sub> Si <sub>2</sub> ) <sub>8h</sub>	4B	6B/2Si	0.0625	−28.15	0.5562	1.0091
Cr:(Si) <sub>4a</sub> :(B) <sub>8h</sub>	4Si	8B	0.125	−38.05	0.5627	1.0209
Cr:(B) <sub>4a</sub> :(B <sub>4</sub> Si <sub>4</sub> ) <sub>8h</sub>	4B	4B/4Si	0.125	−15.76	0.5695	1.0226
Cr:(Si) <sub>4a</sub> :(B <sub>6</sub> Si <sub>2</sub> ) <sub>8h</sub>	4Si	6B/2Si	0.1875	−30.25	0.5743	1.0313
Cr:(B) <sub>4a</sub> :(Si) <sub>8h</sub>	4B	8Si	0.25	−0.89	0.5932	1.0404
Cr:(Si) <sub>4a</sub> :(Si) <sub>8h</sub>	4Si	8Si	0.375	−12.45	0.6078	1.0548

the pure elements at 0 K (bcc-A2 Cr, trigonal-*hR12* B and cubic-A4 Si):

$$\Delta_f E_{\text{Cr}_5\text{B}_{3-x}\text{Si}_x} = E_{\text{Cr}_5\text{B}_{3-x}\text{Si}_x} - 5E_{\text{Cr}} - (3-x)E_{\text{B}} - xE_{\text{Si}} \quad (1)$$

The value of −41.4 kJ/mol for the binary Cr<sub>5</sub>B<sub>3</sub> compound is very close to those reported by other *ab-initio* [46] and CALPHAD extrapolation [47, 48] results. At  $x_{\text{Si}} = 0.0625$  and 0.125, the enthalpy values for 4a substitution of B by Si are systematically lower than for 8h. This result is a clear evidence that Si atoms occupy preferentially the 4a positions.

Some other studies discuss the site occupancies of T2 compounds, as in V–Si–B [17, 26], Ta–Si–B [25], and Nb–Si–B [27]. In particular, the latter study [27] arrived at the conclusion that B in Nb–Si–B tends to form *dumbbell* bonds in the 8h nearest-neighbor positions. Furthermore, as observed in B<sub>14</sub>Ga<sub>3</sub>Ni<sub>27</sub> [49] and Nb<sub>2</sub>OsB<sub>2</sub> [50], for instance, boron atoms have an energetic preference to form short bonds, with interatomic distances varying from 1.40 to 1.90 Å, and can be organized, preferentially, in linear or zigzag infinite chains. In the present work, the *dumbbell* B bonds in the 8h sublattices, as shown in Figure 1, range from 1.68 to 1.82 Å, which are within the expected range. Furthermore, since the *dumbbell* bonds are very stable, only 4a sites remain available for Si occupation. Meanwhile, nearest-neighbor B atoms in 4a sites are weakly bonded, at a distance of approximately 3.8 Å. That fact allows the partial occupation of these positions by Si.

In order to estimate the distribution of Si and B among the sublattices from the DFT calculations, we used Thermo-Calc [51] to calculate the Gibbs energy at 1400°C, employing the enthalpies of formation of the ordered compounds. Within the Compound Energy Formalism (CEF) [52], we adopted the sublattice model (Cr)<sub>5</sub>:(B, Si)<sub>2</sub>:(B, Si)<sub>1</sub>, the last two sublattices corresponding to 8h and 4a, respectively. We used an excess term given by  $y_{\text{B}} y_{\text{Si}} L$ , where  $y_i$  is the site fraction of element  $i$  in the 4a sublattice and  $L$  is a fitting parameter found to be equal to 2808 J/mol of atoms. The enthalpy fit at 1400°C is shown as a solid line in Fig. 4(c), whereas the dashed line corresponds to the Gibbs energy. Both curves are shown only for  $x_{\text{Si}} < 0.125$ , that is, up to full occupation of 4a by Si. Finally, Fig. 4(d) shows the 8h and 4a calculated site occupancies by Si. We obtain therefore a quantitative calculation of Si occupancies showing the preferential nature of Si distribution, showing a reasonable consistency with the Rietveld refined site occupancies, also shown in Fig. 4(d).

In summary, the site occupancies of the T2 phase in the Cr–Si–B system were successfully determined. Synchrotron X-ray diffraction experiments showed that Si occupies preferentially the 4a sites. DFT calculations also pointed to the same conclusion. Moreover, as the sublattice model for a phase in a thermodynamic database must be compatible with other systems, we propose the model (Cr)<sub>5</sub>(B,

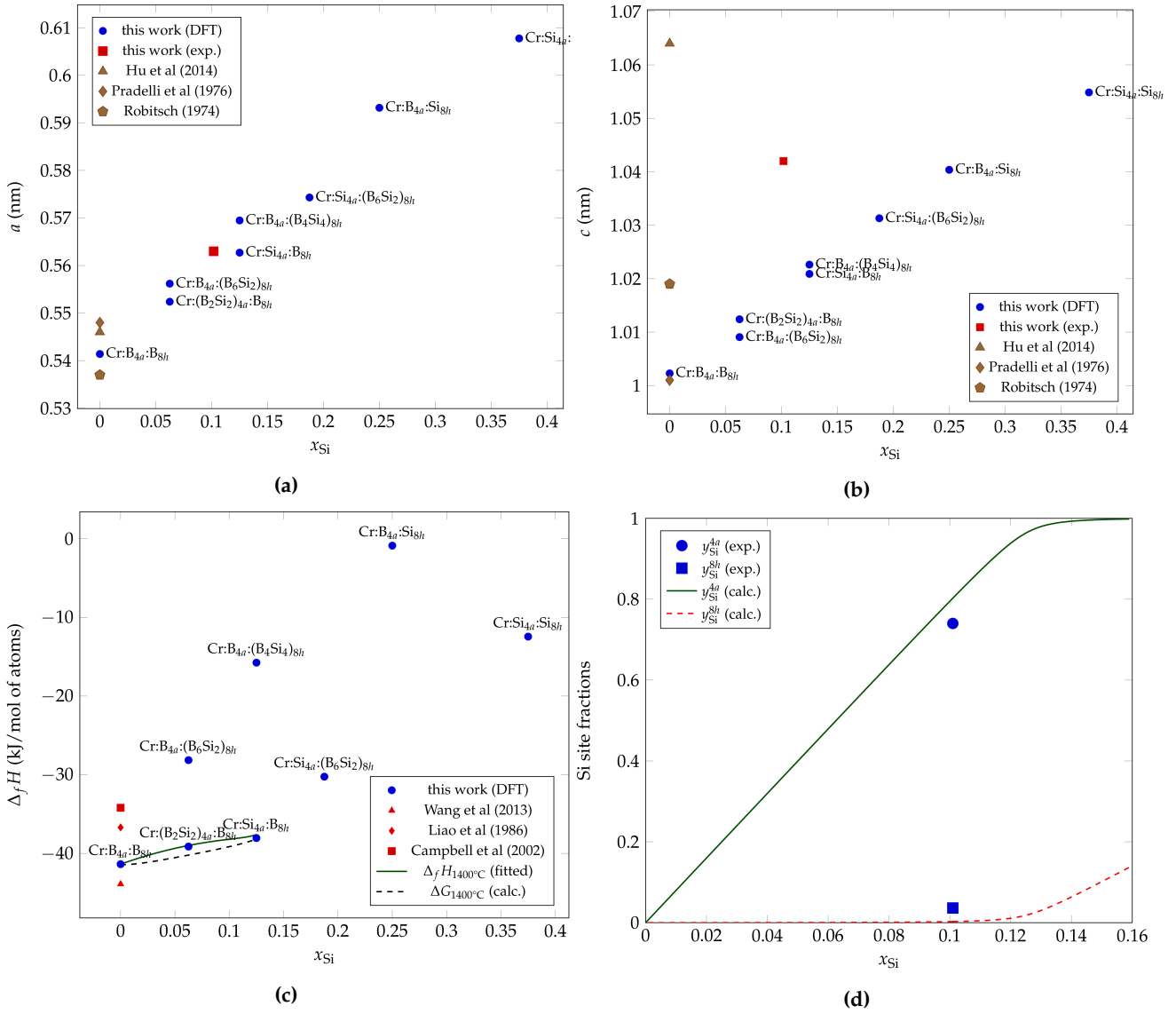


**Figure 4:** Comparison between the lattice parameters  $a$  (a) and  $c$  (b) obtained by DFT calculations, XRD measurements from synchrotron radiation and results from the literature [43–45]. (c) Comparison between the enthalpies of formation at 0 K calculated for several T2 configurations and data from the literature (CALPHAD [47, 48] and *ab-initio* [46]) The full line shows the fit using a CALPHAD model at 1400°C and, in dashed lines, the corresponding Gibbs energy curve. (d) Calculated sublattice occupancies using the CALPHAD model and its comparison with the experimental values in Table 1.

$Si)_2(B, Si)_1$  for the T2 phase in future thermodynamic assessments of relevant systems.

## Acknowledgements

This study was financed in part by the Coordenação de Aperfeiçoamento de Pessoal de Nível Superior (CAPES) - Brasil - Finance Code 001. The financial support of the Fundação de Amparo à Pesquisa do Estado de São Paulo (FAPESP) under Grant No. 2018/10835-6, 2020/08258-0 and 2019/05005-7 is gratefully acknowledged. Finally, the authors acknowledge the Brazilian Synchrotron Light Laboratory (LNLS), Campinas (SP), Brazil, for the high-resolution synchrotron powder diffraction measurements under Project No. 20180142.

## References

- [1] B. P. Bewlay, M. R. Jackson, J. C. Zhao, P. R. Subramanian. *Metall. Mater. Trans. A* 34A (2003) 2043–2052.
- [2] V. O. dos Santos, L. T. F. Eleno, C. G. Schön, K. W. Richter. *Scr. Mater.* 164 (2019) 96–100.
- [3] K. Ito, K. Ihara, K. Tanaka, M. Fujikura, M. Yamaguchi. *Intermetallics* 9 (2001) 591–602.
- [4] K. Ito, M. Kumagai, T. Hayashi, M. Yamaguchi. *Scr. Mater.* 49 (2003) 285–290.
- [5] J. H. Schneibel, M. J. Kramer, D. S. Easton. *Scr. Mater.* 46 (2002) 217–221.
- [6] J. S. Park, R. Sakidja, J. H. Perepezko. *Scr. Mater.* 46 (2002) 765–770.
- [7] R. Sakidja, J. S. Park, J. Hamann, J. H. Perepezko. *Scr. Mater.* 53 (2005) 723–728.
- [8] S. Knittel, S. Mathieu, L. Portebois, S. Drawin, M. Vilasi. *Surf. Coat. Technol.* 235 (2013) 401–406.
- [9] L. Portebois, S. Mathieu, S. Knittel, L. Aranda, M. Vilasi. *Oxidation of metals* 80 (2013) 243–255.
- [10] J. H. Perepezko, R. Sakidja. *Jom* 62 (2010) 13–19.
- [11] D. M. Dimiduk, J. H. Perepezko. *Mrs Bulletin* 28 (2003) 639–645.
- [12] H. Nowotny, A. Wittmann. *Monatsh. Chem.* 89 (1958) 220–224.
- [13] T. F. Villela. Phd thesis (in portuguese), Universidade de São Paulo (USP) (2011).
- [14] V. M. Chad. Phd thesis (in portuguese), Universidade de São Paulo (USP) (2008).
- [15] Z. Sun, Y. Yang, X. Guo, C. Zhang, Y. A. Chang. *Intermetallics* 19 (2011) 26–34.
- [16] R. Sakidja, J. H. Perepezko, S. Kim, N. Sekido. *Acta Mater* 56 (2008) 5223–5244.
- [17] C. Colinet, J.-C. Tedenac. *Intermetallics* 50 (2014) 108–116.
- [18] G. Rodrigues, V. M. Chad, C. A. Nunes, P. A. Suzuki, G. C. Coelho. *Intermetallics* 15 (2007) 241–244.
- [19] K. C. G. Candioto, C. A. Nunes, G. C. Coelho, P. A. Suzuki. *Mater. Charact.* 47 (2001) 241–245.
- [20] M. G. Mendiratta, T. A. Parthasarathy, D. M. Dimiduk. *Intermetallics* 10 (2002) 225–232.
- [21] T. A. Parthasarathy, M. G. Mendiratta, D. M. Dimiduk. *Acta Mater.* 50 (2002) 1857–1868.
- [22] L. Zhang, K. Pan, J. Wang, J. Lin. *Adv. Powder Technol.* 24 (2013) 913–920.
- [23] A. A. A. P. da Silva, N. Chaia, F. Ferreira, et al. *Calphad* 59 (2017) 199–206.
- [24] G. Rodrigues, C. A. Nunes, P. A. Suzuki, G. C. Coelho. *Intermetallics* 12 (2004) 181–188.
- [25] A. U. Khan, C. A. Nunes, G. C. Coelho, et al. *J. Solid State Chem.* 190 (2012) 1–7.
- [26] C. A. Nunes, B. B. de Lima, G. C. Coelho, P. A. Suzuki. *J. Phase Equilib. Diffus.* 30 (2009) 345–350.
- [27] J.-M. Joubert, C. Colinet, G. Rodrigues, et al. *J. Solid State Chem.* 190 (2012) 111–117.
- [28] C. Gianoglio, G. Pradelli, M. Vallino. *Mater. Sci. Technol.* 1 (1983) 51–57.
- [29] P. Villars, A. Prince, H. Okamoto. *Handbook of ternary phase alloys*, vol. 8903. ASM International, Materials Park (OH) (1995).
- [30] H. M. Rietveld. *J. Appl. Crystallogr.* 2 (1968) 65–71.
- [31] R. Rodriguez-Carvajal. In *Abstracts of the Satellite Meeting on Powder Diffraction of the XV Congress of the IUCr*. p. 127.
- [32] O. N. Il'nitskaya, Y. B. Kuz'ma. *Russ. J. Inorg. Chem.* 27 (1982) 1538–1540.
- [33] S. Okada, T. Atoda, I. Higashi. *J. Solid State Chem.* 68 (1987) 61–67.
- [34] P. Hohenberg, W. Kohn. *Phys. Rev.* 136 (1964) B864–B871.
- [35] W. Kohn, L. J. Sham. *Phys. Rev.* 140 (1965) A1133.
- [36] P. Giannozzi, S. Baroni, N. Bonini, et al. *J. Phys.: Condens. Matter* 21 (2009) 395502.
- [37] J. P. Perdew, Y. Wang. *Phys. Rev.* 33 (1986) 8800–8802.
- [38] B. Medasani, M. Haranczyk, A. Canning, M. Asta. *Comput. Mater. Sci.* 101 (2015) 96–107.
- [39] P. Janthon, S. A. Luo, S. M. Kozlov, et al. *J. Chem. Theory Comput.* 10 (2014) 3832–3839. PMID: 26588528.
- [40] P. Janthon, S. M. Kozlov, F. Viñes, J. Limtrakul, F. Illas. *J. Chem. Theory Comput.* 9 (2013) 1631–1640. PMID: 26587624.
- [41] H. J. Monkhorst, J. D. Pack. *Phys. Rev. B* 13 (1976) 5188.
- [42] J. Kreutzer, P. Blaha, U. Schubert. *Comput. Theor. Chem.* 1084 (2016) 162–168.
- [43] G. Pradelli, C. Gianoglio, E. Quadrini. *Rend. Lincei Sci. Fis. Nat.* 65 (1978) 177–184.
- [44] H. Robertsch. *Archiv fuer Lagerstaettenforschung in den Ostalpen* 2 (1974).
- [45] X. Hu, Y. Zhu, N. Sheng, X. Ma. *Sci. Rep.* 4 (2014) 7367.
- [46] B. Wang, D. Y. Wang, Z. Cheng, X. Wang, Y. X. Wang. *Chem. Phys.* 14 (2013) 1245–1255.
- [47] P. K. Liao, K. E. Spear. *Bull. Alloy Phase Diagr.* 7 (1986) 232–237.
- [48] C. E. Campbell, U. R. Kattner. *Calphad* 26 (2002) 477–490.
- [49] M. Tillard, C. Belin. *Inorg. Chem.* 50 (2011) 3907–3912.
- [50] M. Mbarki, R. S. Touzani, B. P. Fokwa. *J. Solid State Chem.* 203 (2013) 304–309.
- [51] J.-O. Andersson, T. Helander, L. Hoglund, P. Shi, B. Sundman. *Calphad* 26 (2002) 273–312.
- [52] M. Hillert. *J. Alloys Compd.* 320 (2001) 161–176.